Fusion Materials

Łukasz Ciupiński
Warsaw University of Technology

Contributions

Materials Modelling

1. Modelling of structure and properties of grain boundaries in iron (WP12-MAT-01-IREMEV-03-02/IPPLM)
2. Formation energy of the σ-phase in the Fe-Mo alloy system (WP12-MAT-01-IREMEV-01-01)

Development of materials and materials technology

3. Development of W-Ta Composites as Long-term Structural Materials (WP12-MAT-01-HHFM-03-01)
4. Optimisation of thermo-mechanical treatment of nano-structured ODS ferritic steel (WP12-MAT-01-ODSFS-01-02)

Materials Characterisation

5. Effect of metallurgical state of samples on the kinetics of the sigma-phase formation in Fe-Cr alloy system (WP12-MAT-01-IREMEV-03-01)
6. Mössbauer spectroscopic study of the miscibility gap in Fe-Cr alloy system (WP12-MAT-01-IREMEV-04-01)
7. Short-Range Order in Fe-rich Fe-Cr Alloys with different thermal history

Modelling of structure and properties of grain boundaries in iron

Motivation

1. Uderstanding mechanisms of GB deformation – behaviour of different types of grain boundaries
2. Data for upper scale models

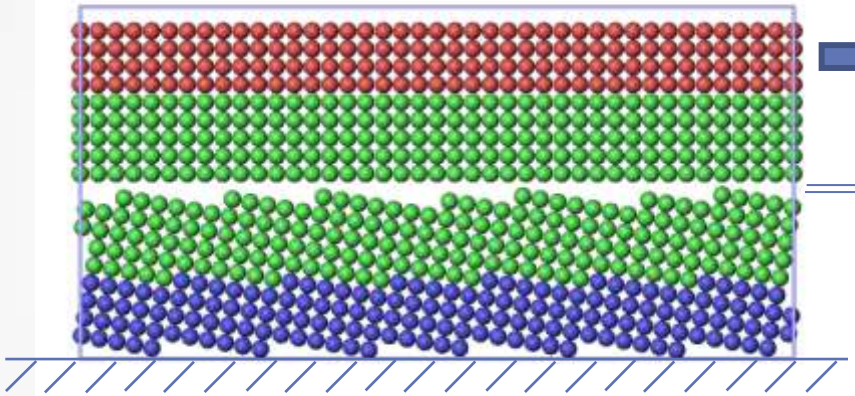

Distance, d

GB shearing - geometry and conditions

Red – X displacement
Green – free
Blue - fixed

Calculation of mechanical parameters

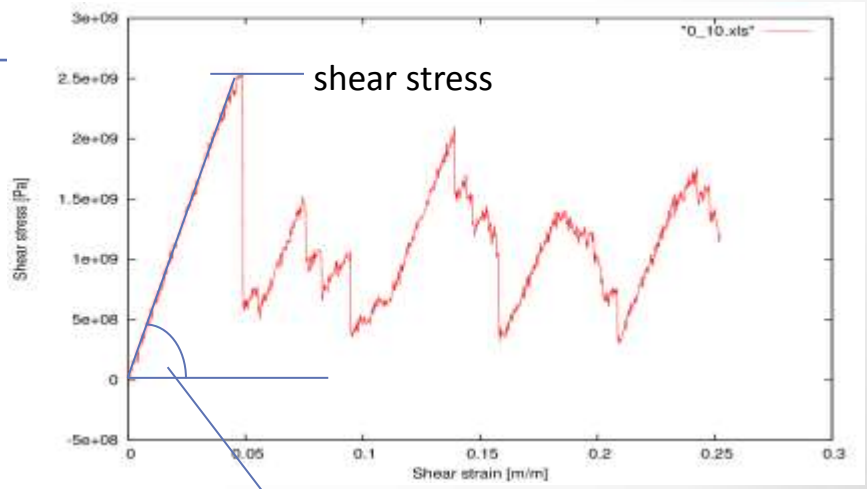

shear modulus

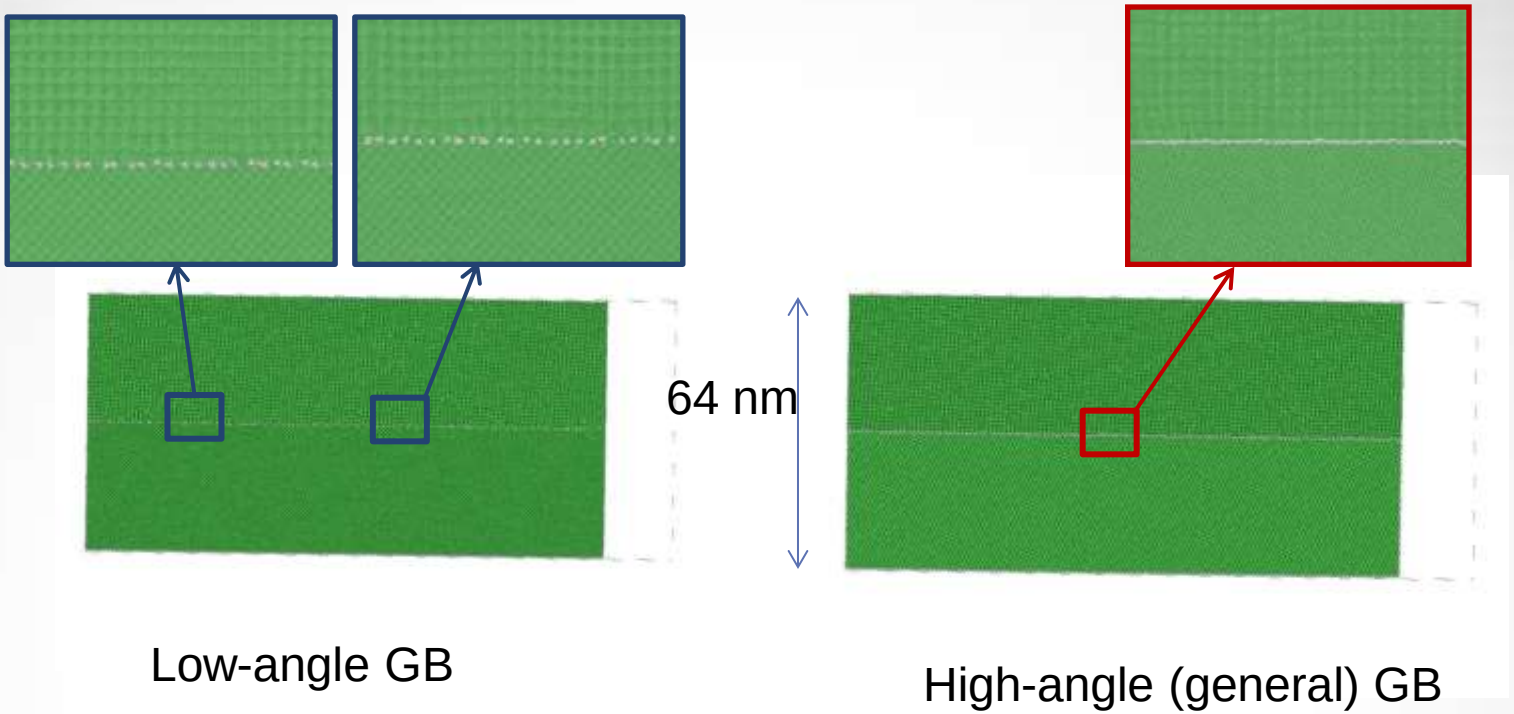

Low-angle GB

High-angle (general) GB

Atomic scale

Molecular Dynamics

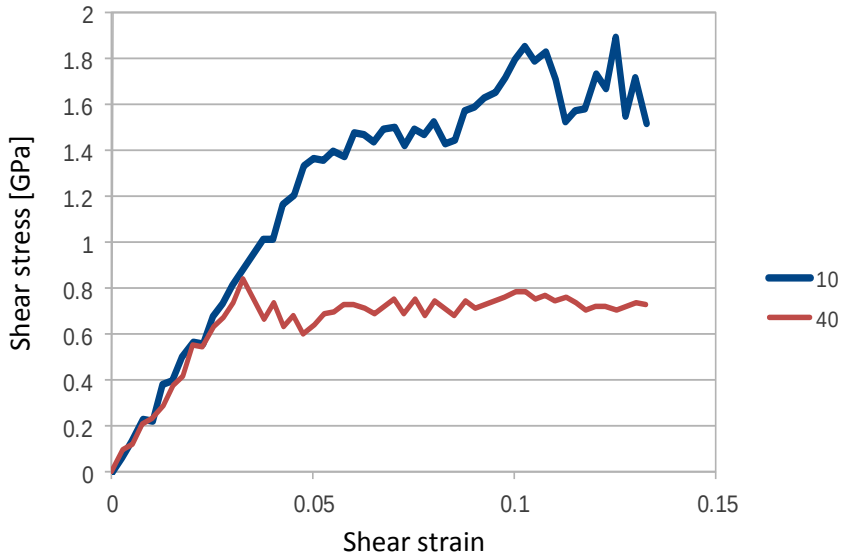

In low angle grain boundaries dislocations are emitted from GB when the system hight is higher than 16 nm

This is not observed in high angle GBs. In high-angle GBs shearing is realized without emmision of dislocations.

Conclusions

1. Shear stress of GBs is much lower than shear stress of single crystal
2. Shear stress and shear modulus are more sensitive to GB surface than misorientation angle (tilt)
3. Low-angle GBs exibits higher shear stress compared to high-angle GBs. The strengthening effect is observed during shearing of low-angle grain boundaries. This is not observed in high-angle grain boundaries
4. In the range we investigated (10^6-10^9) the effect of strain rate on shear stress and shear modulus is not observed
5. Shear stress and shear modulus decreases with temperature

Formation energy of the σ-phase in the Fe-Mo alloy system

Goals, Samples & Method

The aim of this task was to calculate : (a) formation energy, (b) configurational and (c) magnetic entropies, and (d) distribution of atoms over sublattices in σ-phase Fe-Mo alloys.

Two model alloys were considered: (1) Fe_{17} Mo_{13} and (2) $Fe_{13}Mo_{17}$. The former is designated as σ-21824 and the latter as σ-20812. (the figures after σ stand for the number of Fe atoms at the sublattices (sites) A, B, C, D, E, respectively)

The calculations were carried out within the Korringa–Kohn–Rostoker (KKR) - Coherent Potential Approximation (CPA) method.

Results

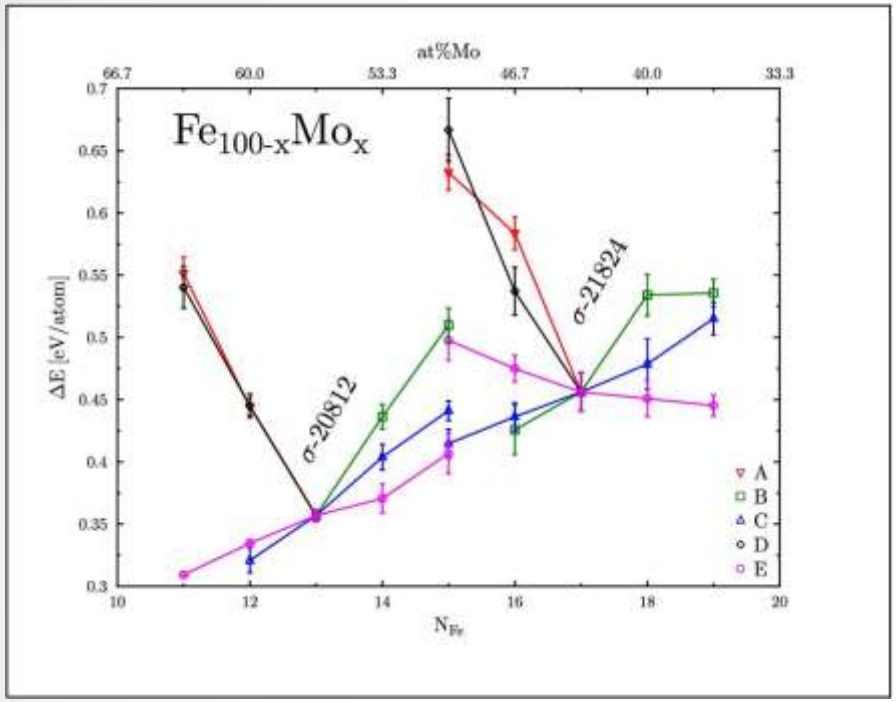

Fig. 1 Difference of the formation energy for the two chosen configurations (samples) of the σ-phase Fe-Mo (relative to α), ΔE, versus the number of Fe atoms per unit cell, N_{Fe}. Mo concentration is also indicated.

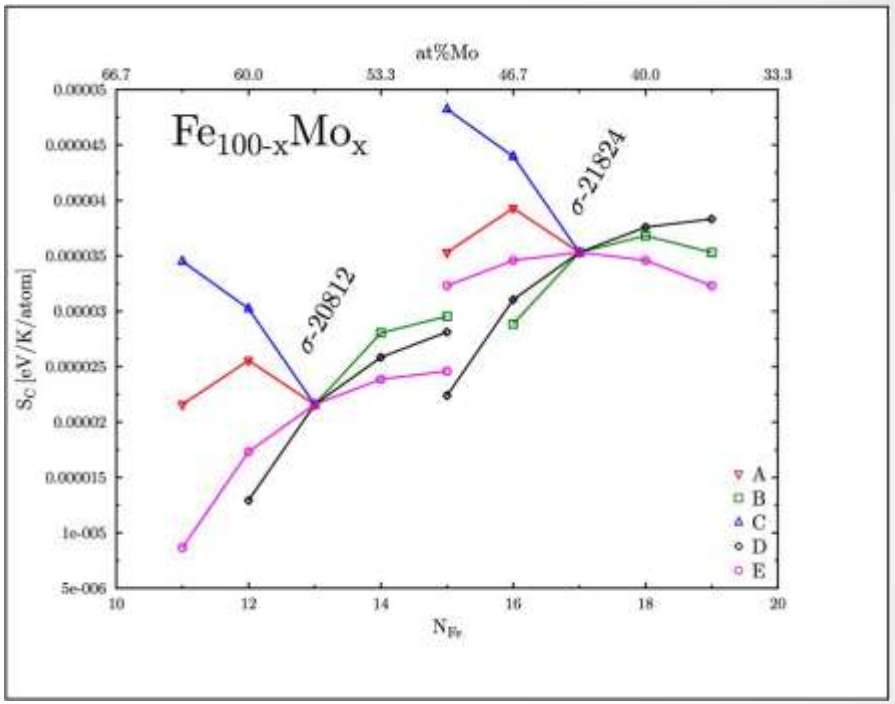

Fig. 2 Configuration entropy, S_C vs. the number of Fe atoms per unit cell, N_{Fe}, for different samples) and, within each sample, for all five sites. The concentration of molybdenum is indicated, too

Conclusions

- Formation energy of the σ-FeMo, ΔE, increases with Fe content from ~ 0.36 eV/atom for $Fe_{13}Mo_{17}$ to ~0.46 eV/atom for $Fe_{17}Mo_{13}$

- For a given sample ΔE is characteristic of a given lattice site, and it depends strongly on the number of Fe atoms, $N_{Fe,}$ in a unit cell.

- Similar dependence on the composition, and for a given composition on the lattice site and $N_{Fe,}$ has the configurational entropy, S_C, but its values are in the range of several μeV/atom.

- The magnetic entropy, S_M, being of the same order of magnitude as S_C , exhibits also a strong dependence on the alloy composition and $N_{Fe,}$ but it hardly depends on the lattice site.

Development of W-Ta Composites as Long-term Structural Materials

Motivation

Although, tungsten seems to be the best candidate for plasma facing material one of the main obstacles of tungsten use is its low ductility and fracture toughness at room temperature.

Goal

Fabricate dens and tough tungsten composites via Pulse Plasma Sintering of powders

Materials

W-Ta powder mixtures after mechanical alloying, 2 nd 10 wt.% of Ta in form of powder and short fibre (3 mm)

Results

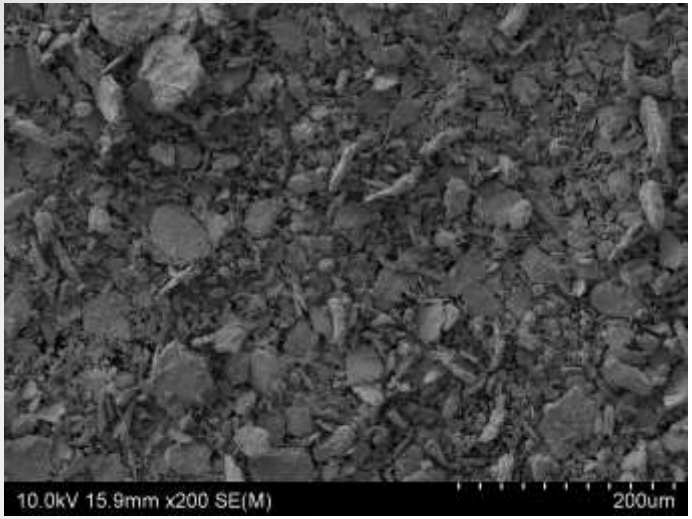

W (MA 1h - 170RPM) + 10%powder
Turbula 1h/90RPM (as delivered by IST)

sample	Density (g/cm^3)	% TD
1 - W + 10% Ta Fiber	18.7	**98.4**
2 - W + 2% Ta Fiber	18.1	94.1
3 - W + 2% Ta Powder	18.1	94.3
4 - W + 10% Ta Powder	18.4	97.0
5 - W (MA)	18.0	93.4
6 - W Pristine	17.3	89.8

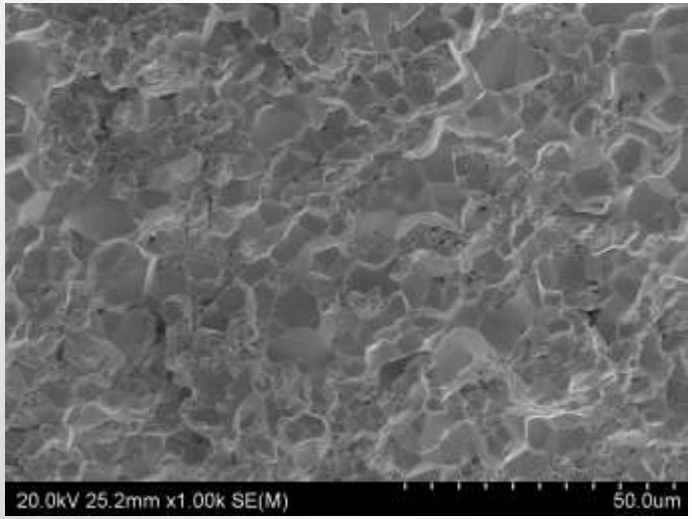

Fracture surface, W + 10% Ta fibre

Conclusions

- Pulse Plasma Sintering method can be successfully employed to fabricate high density W-Ta composites
- The highest density has been achieved for W Ta (10%fiber) - 98.4% TD.
- The milling process (MA) of tungsten powder leads to sinters grain size reduction and higher sinter density.
- The distribution of Ta powders seems uniform while the Ta fibres not

Optimisation of thermo-mechanical treatment of nano-structured ODS ferritic steel

Aim

To determine the influence of HIP pressure on tensile properties of the 14Cr ODS ferritic steel

Fe-14Cr-2W-0.3Ti-0.3Y_2O_3

(elemental powders)

- mechanical alloying in a planetary ball mill in hydrogen atmosphere
- degassing
- HIPping at 1150°C under pressure in the range of 185 – 300 MPa

Results

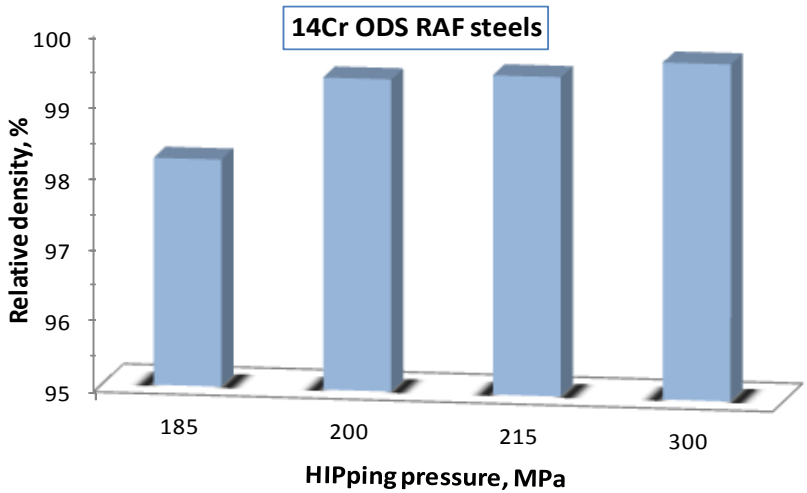

- **with increasing the isostatic pressure the density of specimens also increases**
- **it is difficult to obtain fully dense ODS alloy after HIPping only**

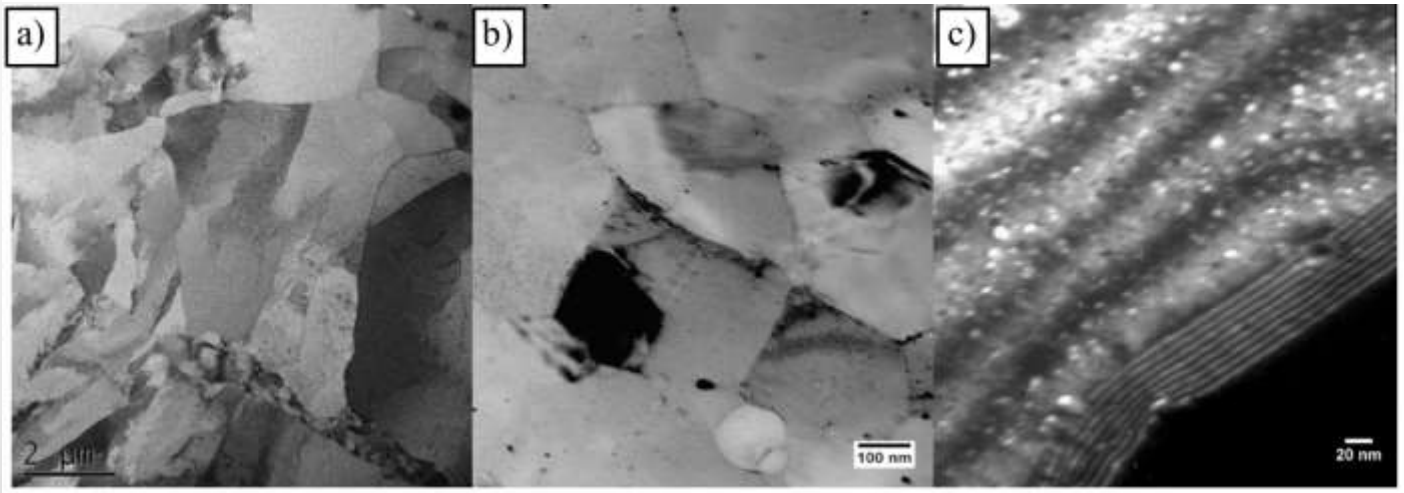

TEM images of the as-HIPped ODS ferritic steels, a) general view, b) higher magnification and c) dark field TEM image of nanoparticles.

Results

Microhardness of the ODS ferritic steel HIPped at 1150°C for 4 h under various pressure

$\mu HV_{0.1}$ ODS steel	HIPped at 185 MPa	HIPped at 200 MPa	HIPped at 300 MPa
	362±15	370±16	380±12

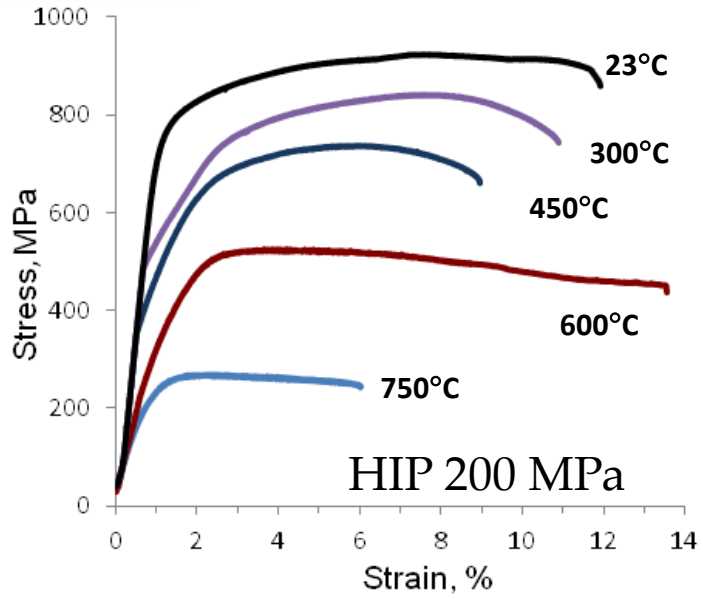

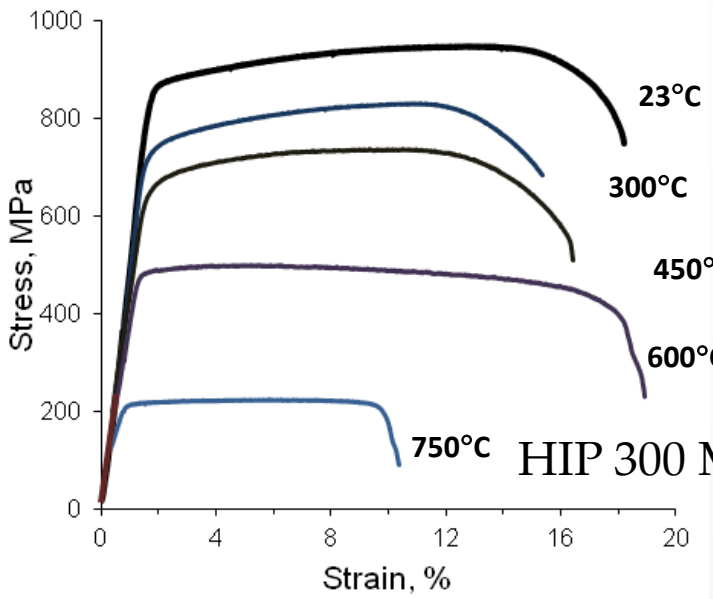

- **no significant differences in the strength (UTS and YS)**
- **lower total elongation for material HIPped under lower pressure**

Conclusions

1. With increasing the isostatic pressure the density of the ODS steel also increases, however a residual porosity was observed in all tested materials.
2. Specimens after HIPping under various pressure have similar microstructure which consists of bimodal-size grains, low dislocation density and large number of oxide particles, with a size about a few hundred of nano-meters and usually located at the grain boundaries.
3. The HIPping pressure in the range between 185-300 MPa has negligible influence on the hardness and tensile strength of the ODS steel, however with increasing the isostatic pressure the total elongation of tested materials significantly increases.

Mössbauer Spectroscopy Studies of Fe-Cr alloys

Motivation

- Fe-Cr-based steels are good candidates for design of various structural components in advanced nuclear energy installations such as Generation IV and fusion reactors

- At elevated temperatures, high-chromium steels are not stable:
  - (1) the phase decomposition (PD) into the Fe-rich (α) and the Cr-rich (α') phases at T < ~500°C leads to the so-called miscibility gap (MG), and
  - (2) the precipitation of the σ-phase that at T > ~500°C

→ an enhancement of embrittlement

- Interest :
  - (a) underlying mechanism(s),
  - (b) borders of MG i.e. the composition of α and α' phases, (c) kinetics of decomposition
  - (d) short-range ordering (SRO)

Mössbauer Spectroscopy Studies of Fe-Cr alloys

- Miscibility gap in Fe-Cr alloy (phase decomposition into the Fe-rich (α) and the Cr-rich (α') phases)
  - Fe-Cr14 EFDA sample (xCr=15.15 at%)
  - isothermal vacuum annealing at 415 and 450°C

- Effect of thermal history of samples on SRO in Fe-Cr
  - Series of $Fe_{1-x}Cr_x$ samples with x <◎20
  - Three different heat treatments T1, T2, T3

- Effect of metallurgical state of samples on ◎◎◎ phase transformation kinetics in Fe-Cr
  - Two series of $Fe_{54}Cr_{46}$ were studied: (a) bulk, plastically deformed by cold-rolling (10-60% deformation), (b) foils (25◎m) with a deformation degree of 77-97%
  - transformation to ◎ was done by isothermal annealing at 700°C

Mössbauer Spectroscopy Studies of Fe-Cr alloys

Effect of thermal history of samples on SRO in Fe-Cr

- Heat treatments:
  - T1 – annealing at 800 °C for 3 h in argon, followed by quenching in liquid nitrogen (homogenization)
  - T2 – annealing at 800 °C for 20 h in argon, followed by 2h annealing at 520 °C. Afterwards, the temperature was slowly (20 h) decreased down to 430 °C at which temperature the samples were kept for 12 h. Finally, the quartz tube was removed quickly from the furnace and the samples thrown on a block of brass kept in the cool zone of the tube
  - T3 – vacuum annealing at 415 °C for different periods followed by a cooling in the tube removed from the furnace (only x=15.15 at%)

Miscibility gap in Fe-Cr alloy

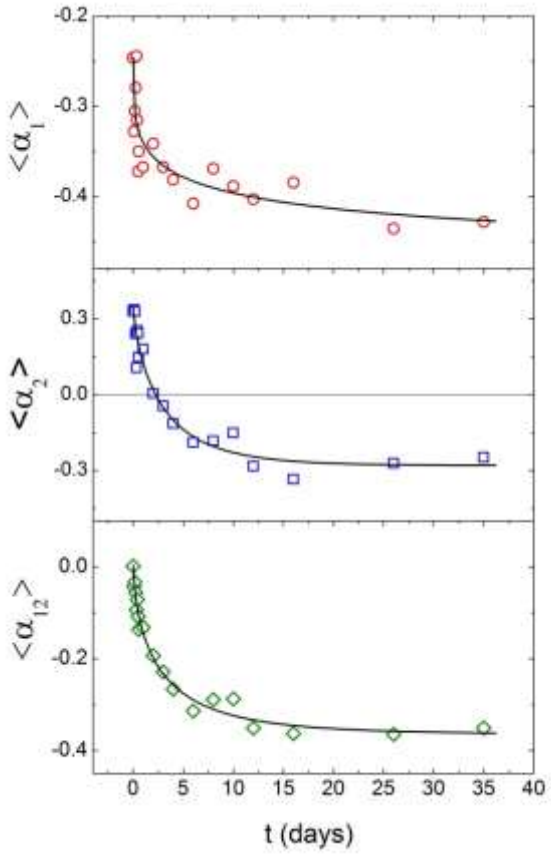

- SRO parameters for 1NN, 2NN and 1NN+2NN shells were determined as a function of annealing time, and shown to follow the JMAK equation
- The kinetics of PS was quantitatively described in terms of the JMAK equation.
- The activation energy for PS was determined as 122 kJ◎mol

SRO-parameters versus the annealing time, *t*, at 415°C. The solid lines - fit to the Johnson-Mehl-Avrami-Kolgomorov (JMAK) equation.

Effect of thermal history of samples on SRO in Fe-Cr

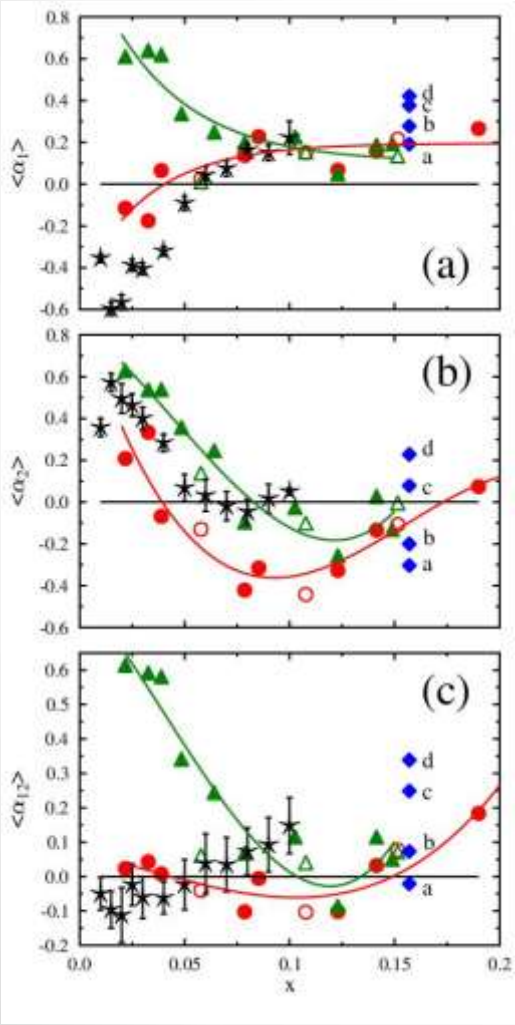

- SRO parameters are characteristic of a given atomic shell (1NN, 2NN), and for a given shell they significantly depend on the applied heat treatment
- Distribution of Cr atoms in the homogenized samples is not random, the departure from randomness particularly large for low-concentrated samples where a high degree of Cr atoms depletion within the 1NN-2NN zone around Fe atoms was revealed
- Evidence for a clear-cut inversion was found for $Fe_{85}Cr_{15}$ sample that underwent a prolonged annealing at 415°C

SRO in Fe-Cr: T1 – triangles, T2 – circles (open - EFDA samples)
T3 – diamonds (blue), Ref.2 - asterisks

Effect of metallurgical state of samples on σ-phase kinetics in Fe-Cr

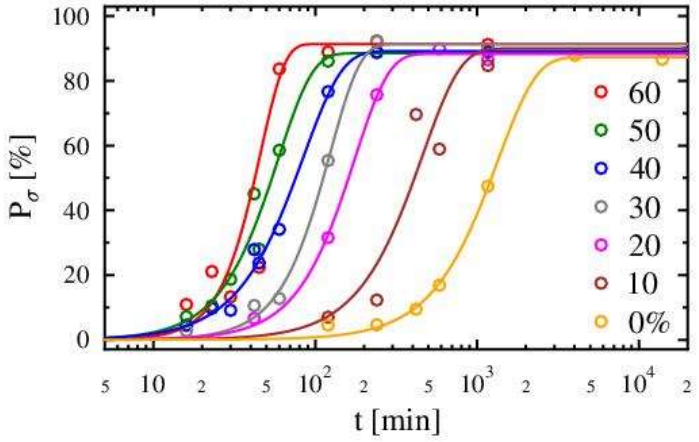

σ-phase kinetics - bulk samples

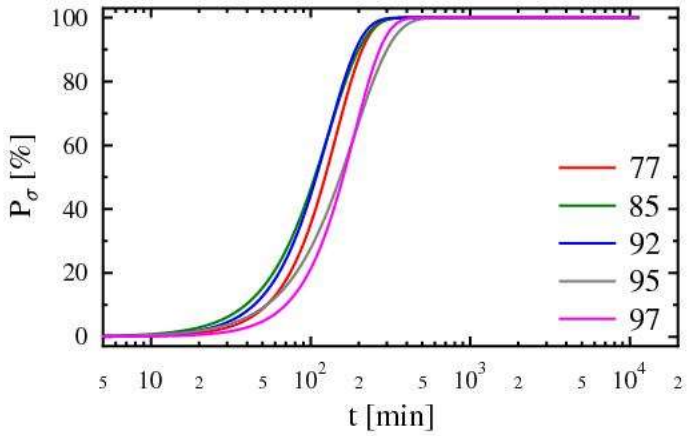

σ-phase kinetics - foil samples

- Influence of internal strain caused by plastic deformation (cold rolling) on the kinetics of σσσ phase transformation was shown to be strong
- Avrami exponent, thus the transformation's mechanism does not meaningfully depend on the deformation degree
- The rate constant, hence the activation energy, depends not only on the degree of deformation but also on the thermal history of the samples

Thank you for your kind attention !

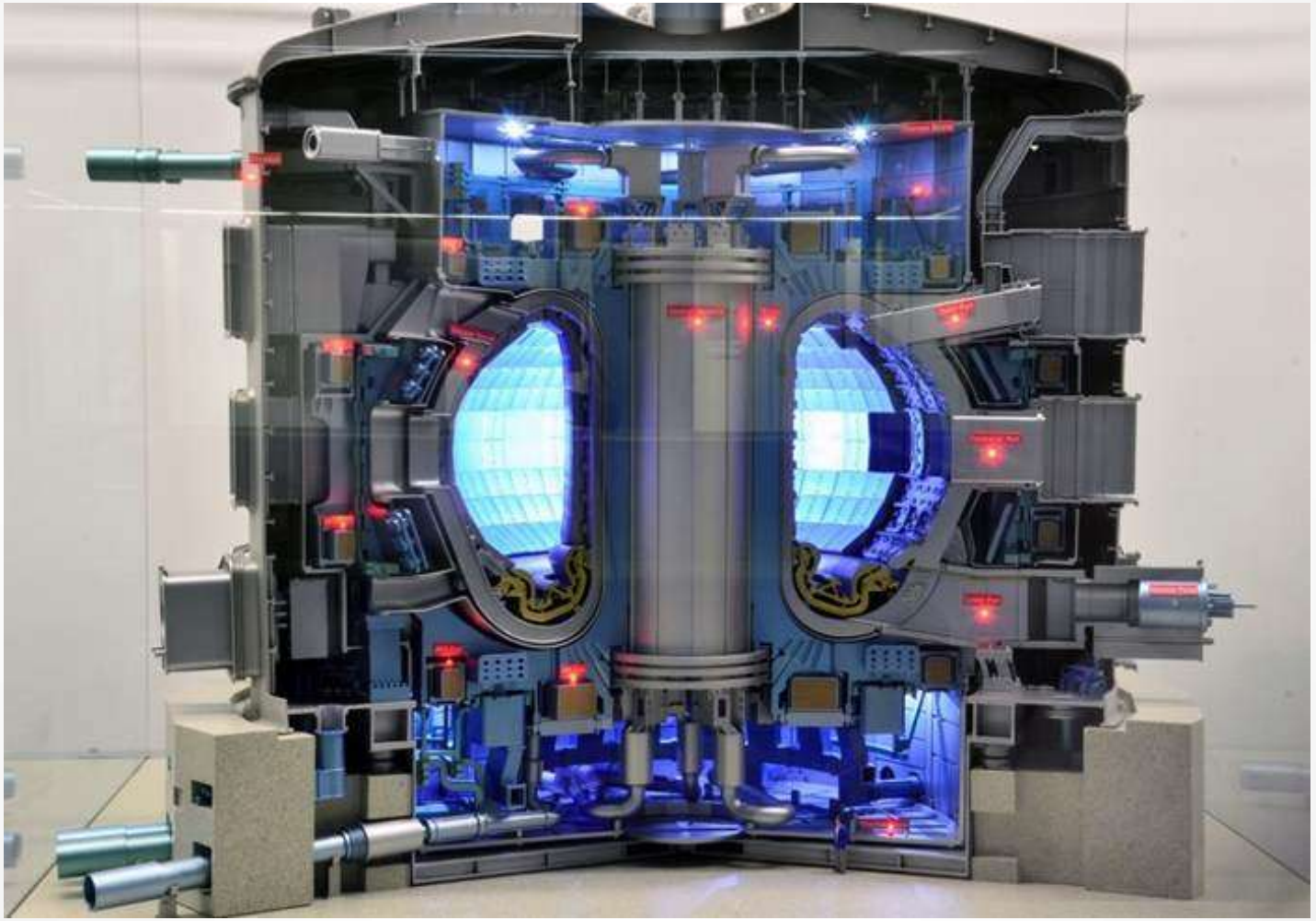

Source: http://news.sciencemag.org